Medicinal Chemistry Research
https://doi.org/10.1007/s00044-020-02611-7

MEDICINAL CHEMISTRY RESEARCH

ORIGINAL RESEARCH

Propargylated monocarbonyl curcumin analogues: synthesis, bioevaluation and molecular docking study

Amol A. Nagargoje[1,2] · Satish V. Akolkar[1] · Dnyaneshwar D. Subhedar[1] · Mubarak H. Shaikh[1,3] · Jaiprakash N. Sangshetti[4] · Vijay M. Khedkar[5] · Bapurao B. Shingate[1]

Received: 21 April 2020 / Accepted: 31 July 2020

Abstract

In the current experimental study, we have synthesised new monocarbonyl curcumin analogues bearing propargyl ether moiety in their structure and evaluated for in vitro antifungal and radical scavenging activity. The antifungal activity was carried out against five human pathogenic fungal strains such as *Candida albicans*, *Fusarium oxysporum*, *Aspergillus flavus*, *Aspergillus niger* and *Cryptococcus neoformans*. Most of the curcumin analogues displayed excellent to moderate fungicidal activity when compared with standard drug Miconazole. Also, synthesised analogues exhibited potential radical scavenging activity as compared with standard antioxidant Butylated hydroxyl toluene (BHT). Based on biological data, structure-activity relationship (SAR) were also discussed. Furthermore, in silico computational study was carried out to know binding interactions of synthesised analogues in the active sites of enzyme sterol 14α-demethylase (CYP51).

Graphical Abstract

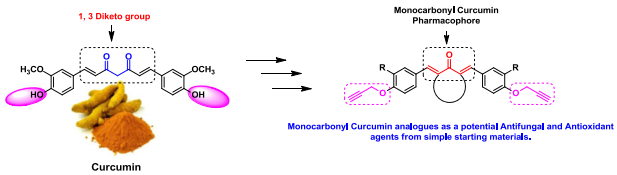

Keywords Monocarbonyl curcumin analogues · Antifungal activity · Antioxidant activity · SAR · Molecular docking study

Introduction

Curcumin is the principal curcuminoid of the turmeric plant of the family *Zingiberaceae*. It has been used to treat many health conditions in India and other parts of Asia since ancient times. According to recent literature, curcumin is the multi-target pleiotropic agent displaying a wide spectrum of biological activities (Goel et al. 2008; Marchiani et al. 2013; Bairwa et al. 2014; Shetty et al. 2015). Curcumin has been evaluated in clinical trials for the treatment of various diseases like cancer, liver diseases, infectious diseases and rheumatoid arthritis (Hatcher et al. 2008; Bairwa et al. 2014). However, clinical use of the curcumin is restricted due to poor bioavailability, poor

Supplementary information The online version of this article (https://doi.org/10.1007/s00044-020-02611-7) contains supplementary material, which is available to authorized users.

✉ Bapurao B. Shingate
bapushingate@gmail.com

[1] Department of Chemistry, Dr Babasaheb Ambedkar Marathwada University, Aurangabad 431004, India

[2] Department of Chemistry, Khopoli Municipal Council College, Khopoli 410203, India

[3] Department of Chemistry, Radhabai Kale Mahila Mahavidyalaya, Ahmednagar 414001, India

[4] Department of Pharmaceutical Chemistry, Y. B. Chavan College of Pharmacy, Rafiq Zakaria Campus, Aurangabad 431001, India

[5] Department of Pharmaceutical Chemistry, School of Pharmacy, Vishwakarma University, Pune 411048, India

Published online: 10 August 2020

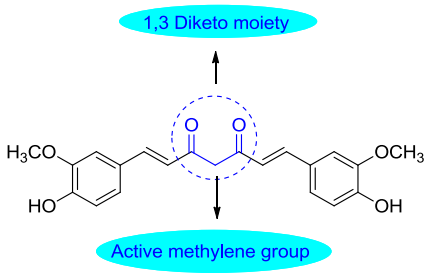

Fig. 1 Curcumin and groups responsible for the instability

pharmacokinetics and rapid in vivo metabolism (Anand et al. 2008). It was observed that, presence of the β-diketone and active methylene groups are responsible for the instability of curcumin (Anand et al. 2007; Wang et al. 1997) (Fig. 1).

Structural modification on curcumin by replacing β-diketone moiety as well as an active methylene group with single keto-functionality leads to the formation of therapeutically active, stable monocarbonyl analogues of curcumin (MACs) (Shetty et al. 2015). The literature survey revealed that, MACs were displayed a wide spectrum of biological activities which are found to be superior to curcumin itself. MACs shows potential anticancer (Kerru et al. 2017), anti-inflammatory (Wang et al. 2017), antioxidant (Zheng et al. 2017), antibacterial (Sanabria-Rios et al. 2015), anti-Alzheimer's activity (Chen et al. 2011), antiparasitic (Carapina da Silva et al. 2019), antileishmanial (Tiwari et al. 2015), topoisomerase II alpha inhibitors (Paul et al. 2014), antiobesity (Buduma et al. 2016), anti-tubulin (Singh et al. 2016), anti-invasive chemotypes (Roman et al. 2015), lipoxygenase and proinflammatory cytokines (Ahmad et al. 2014), anti-tubercular (Subhedar et al. 2017), antifungal activity (Sahu et al. 2012) etc.

In recent years, invasive fungal infections are a major concern due to an increase in organ transplantation, stem cell transplantation, chemotherapy and human immunodeficiency virus. Candidosis, aspergillosis and cryptococcosis, are three major fungal infections responsible for clinical infections in patients having a weak immune system. Although, there are several drugs available to treat fungal diseases, multidrug-resistant strain development among the fungal species against existing amphotericin B, triazoles, and echinocandins based antifungal drugs (Pappas et al. 2015) become a critical problem for therapeutic strategies (Seufert et al. 2018). Also, existing antifungal drugs have many side effects. Long term use of the existing antifungal drugs can induce many side effects such as cough, bad taste, nausea, hepatotoxicity, liver toxicity, hypokalemia, fever, gastrointestinal, endocrinologic, metabolic, carcinogenic, chills and drug-drug interactions between azole and other drug classes that are metabolised *via* similar pathways in the liver (Bodey 1992; Shehaan et al. 1999).

These limitations emphasise the need to develop new and more effective antifungal agents. Martins et al. (Martins et al. 2009) evaluated the potential of curcumin against various fungal strains as an effective antifungal as compared with commercial drug fluconazole. Very recently, anti-infective properties of curcumin have been reviewed (Praditya et al. 2019). Hence, curcumin and its analogues can be the new scaffold in the search of new antifungal agents. Covalent modification by prenylation have been recognised as a mechanism for promoting membrane interactions and biological activity of a variety of cellular proteins (Casey 1992).

It was observed that, reactive oxygen species were involved in the mechanism of action of antifungal drugs (Da Silva et al. 2014). Therefore, new antifungals with antioxidant potential can be a good choice. Literature revealed that, curcumin moiety is responsible for antioxidant activity (Masuda et al. 2001; Sokmen, Khan 2016). Considering the antioxidant activity of curcumin analogues (Li et al. 2015; Sahu et al. 2016a, b; Lal et al. 2016; Zheng et al. 2017), many attempts were made to develop new curcumin based molecules as an antioxidant agents. Some of the representative structures of the molecules as an antioxidant agents were shown in Fig. 2.

Under this context and as a part of our ongoing research in the synthesis and biological evaluation of monocarbonyl curcumin analogues (Deshmukh et al. 2020; Subhedar et al. 2017; Nagargoje et al. 2019, 2020), we report herein, synthesis, antifungal and antioxidant evaluation of new propargylated monocarbonyl curcumin analogues. Furthermore, to understand the binding mechanism of newly synthesised analogues into the active sites of cytochrome P450, molecular docking study was also performed.

Results and discussion

Chemistry

In the present work, we have described the synthesis of new propargylated monocarbonyl curcumin analogues by the Claisen–Schmidt type condensation (Fine, Pulaski 1973; Ziani et al. 2013) of propargylated benzaldehydes with monoketone linkers like cyclohexanone, cyclopentanone, acetone and 4-methyl piperidone by literature method. The reaction of benzaldehyde **1a–c** with propargyl bromide in the presence of an alkaline condition resulted in the corresponding substituted prop-2-yn-1-yloxy-benzaldehydes **2a–c** in excellent yields (Scheme 1). The condensation of these benzaldehydes **2a–c** with respective monoketone **3a–d** using aq. NaOH and ethanol at room temperature resulted into corresponding propargylated monocarbonyl curcumin analogues **4a–i** in a good yield. (Scheme 1).

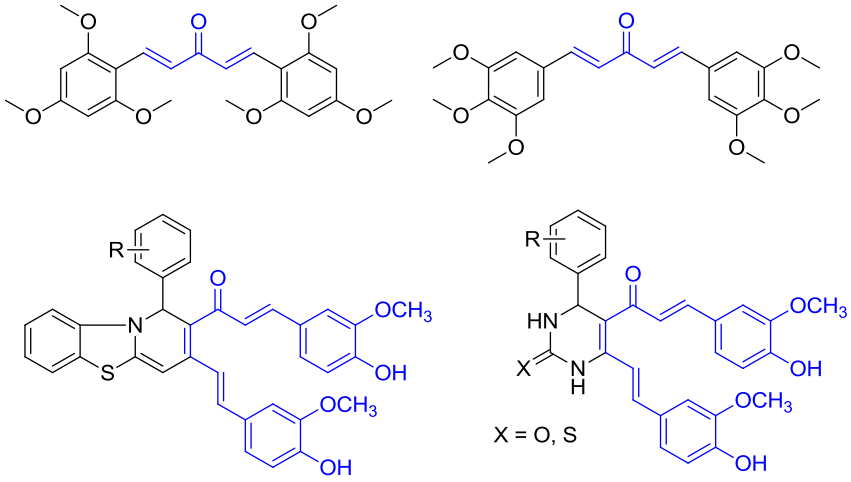

Fig. 2 Known MACs with antioxidant activity

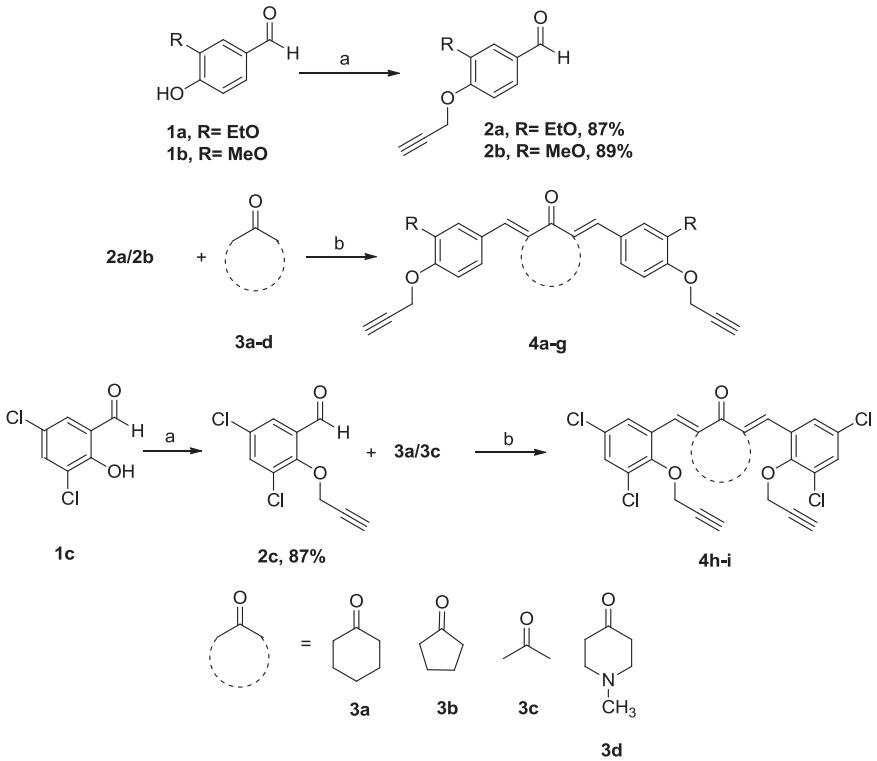

Scheme 1 Synthesis of propargylated monocarbonyl curcumin analogues. Reagent and conditions: (a) Propargyl bromide, K_2CO_3, DMF, rt, 3–4 h; (b) Aq. NaOH, EtOH, rt, 4–5 h

The formation of propargylated monocarbonyl curcumin analogues **4a–i** has been confirmed by physical data and spectroscopic methods such as FT-IR, ^{1}H NMR, ^{13}C NMR and LC/ESI-MS. According to the FT-IR spectrum of compound **4a**, the peaks observed at 3262 cm^{-1}, 2120 cm^{-1} indicate the presence of the alkyne group and 1660 cm^{-1} for the presence of a carbonyl group. In the ^{1}H NMR spectrum of compound **4a**, the triplet at 1.47 ppm is observed for methyl group adjacent to a methylene group present on the benzene ring, multiple ranging in between 1.84 and 1.78 ppm, and triplet at 2.93 ppm is observed for methylene groups of cyclohexanone ring, triplet at 2.53 ppm with coupling constant 2.4 Hz for two alkyne protons (This indicates coupling of acetylinic proton with methylene protons adjacent to oxygen and alkyne group), the quartet at 4.12 ppm for four methylene protons adjacent to oxygen and methyl group on benzene rings, a doublet at 4.81 ppm with coupling constant 2.4 Hz (This indicates coupling of these protons with terminal acetylene protons) for the presence of two methylene protons adjacent to oxygen and alkyne group on a benzene ring. In addition to this, the signal appeared at 7.03 and 7.08 ppm for six aromatic protons of benzene rings. The signal appeared at 7.73 ppm is for two alkene protons. These alkene protons are benzylidine protons, and also in β position to the carbonyl group, hence due to resonance effect and –I effect of the

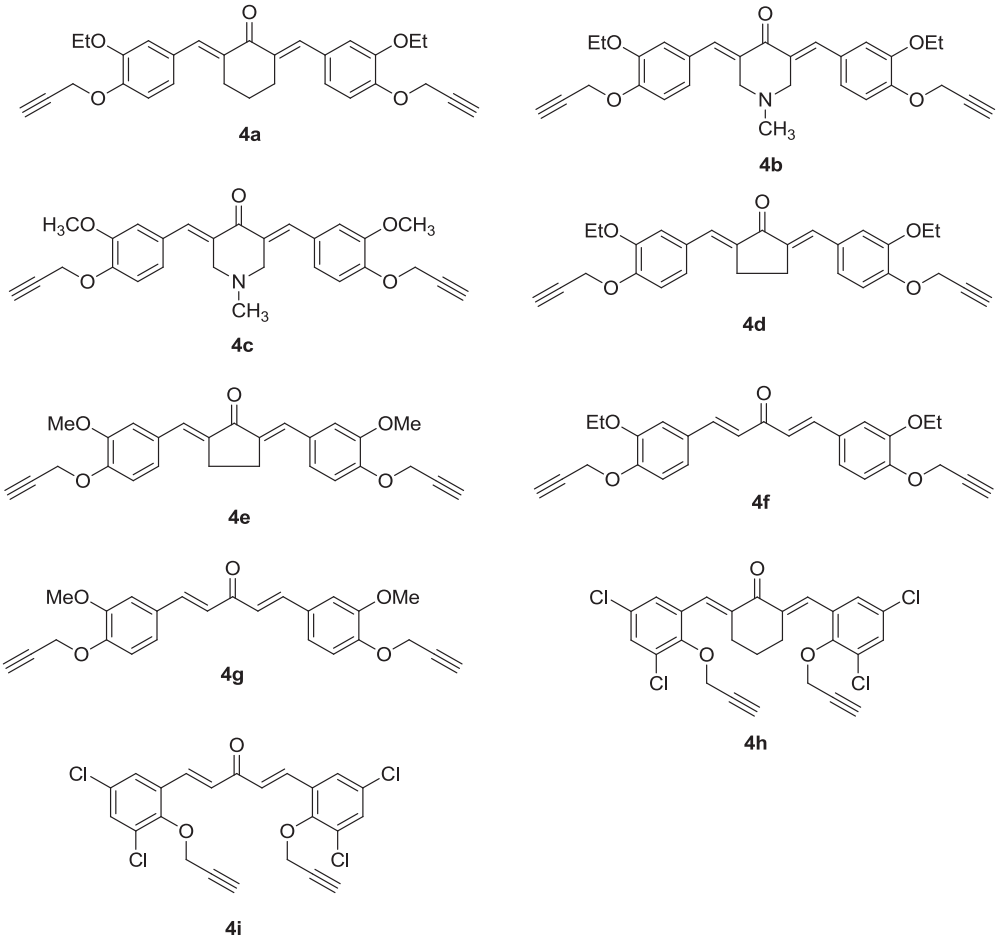

Fig. 3 Structures of synthesised monocarbonyl curcumin analogues

carbonyl group and benzene ring this signal is shifted to downfield region. In the ^{13}C NMR spectrum of compound **4a**, the signal at 14.8 ppm is observed for the methyl carbon and the signals at 23.0 and 28.5 ppm indicate the presence of two methylene carbon of cyclohexanone ring. The signals at 56.8 and 64.6 ppm indicate the presence of methylene carbons adjacent to oxygen. The signal at 76.0 and 78.4 ppm shows the presence of alkyne carbons. Furthermore, the peak observed at 190.1 ppm for carbonyl carbon. The formation of compound **4a** has been further confirmed by mass spectrometry. The calculated $[M\text{-}H]^+$ for compound **4a** is 469.2093 and observed $[M\text{-}H]^+$ in the mass spectrum at 469.2143. Similarly compounds **4b–i** were characterised by the spectral analysis. The structures of all the synthesised MACs are given in Fig. 3.

In vitro antifungal activity

The synthesised MACs were evaluated for in vitro antifungal activity against various fungal strains like *Cryptococcus neoformans*, *Aspergillus niger*, *Aspergillus flavus*, *Candida albicans*, *Fusarium oxysporum* etc. The minimum inhibitory potential of synthesised analogues were compared against the standard antifungal drug Miconazole. The *MIC* values in µg/mL were estimated and the results are summarised in Table 1.

Most of the synthesised MACs exhibited excellent to moderate antifungal potential against most of the pathogenic fungal strains, which is reflected by their *MIC* values. Antifungal activity of synthesised MACs compare to standard Miconazole is represented graphically in Fig. 4. Among the series, compound **4a** displayed equivalent or two/three fold more potency as compared with positive control Miconazole, which reflects its broad-spectrum nature. Compound **4a** demonstrates excellent inhibitory activity against *Candida albicans, Fusarium oxysporum* and *Cryptococcus neoformans* (*MIC* 12.5 µg/mL, *MIC* 12.5 µg/mL and *MIC* 12.5 µg/mL, respectively) with compared with Miconazole. Also, **4a** is equipotent against *Aspergillus flavus and Aspergillus niger* (*MIC* 25 µg/mL each) with compared with Miconazole. Furthermore, compound **4b** and **4c** exhibited almost equal potency as

Table 1 In vitro antifungal and antioxidant evaluation of propargylated monocarbonyl curcumin analogues

Entry	Antifungal activity (MIC in μg/mL)					Molecular docking score	Antioxidant activity (IC_{50} in μg/mL)
	CA[a]	FO[b]	AF[c]	AN[d]	CN[e]		
4a	12.5	12.5	25	25	12.5	−8.939	24.28 ± 0.45
4b	25	12.5	25	25	50	−8.559	16.17 ± 0.11
4c	62.5	25	37.5	12.5	25	−8.097	15.78 ± 0.47
4d	37.5	87.5	25	50	62.5	−8.534	40.34 ± 0.14
4e	25	25	75	50	100	−7.490	13.18 ± 0.34
4f	75	75	12.5	25	75	−7.762	28.36 ± 0.43
4g	100	75	75	100	175	−7.338	27.81 ± 0.05
4h	12.5	25	75	100	25	−7.637	41.42 ± 0.67
4i	150	125	150	175	100	−7.088	12.78 ± 0.71
MA	25	25	12.5	25	25	–	–
BHT	–	–	–	–	–	–	16.47 ± 0.18

MA miconazole, *BHT* butoxy hydroxy tolune

[a]Candida albicans

[b]Fusarium oxysporum

[c]Aspergillus flavus

[d]Aspergillus niger

[e]Cryptococcus neoformans

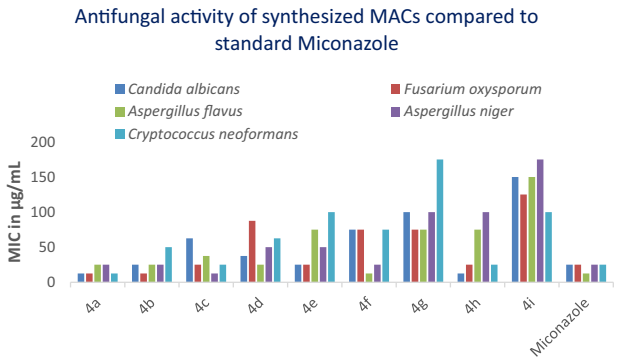

Fig. 4 Antifungal activity of synthesised MACs compared with Miconazole

compared with standard. Compound **4e**, **4f** and **4h** displayed moderate potential to act as an antifungal agent. Also, antifungal activity data showed that **4a**, **4b** and **4f** were the most active against *Aspergillus flavus*. The trends in the *MIC* values of the synthesised analogues help to establish some sort of structure-activity relationship (SAR). From the minimum inhibitory concentration values of the synthesised propargylated monocarbonyl curcumin analogues against different fungal strains, it was observed that curcumin analogues with cyclic linkers like cyclohexanone and *N*-methyl piperidone enhances antifungal potential. To be more specific, analogues with cyclohexanone linker displayed better antifungal activity. Comparing *MIC* values of compound **4a** and **4h** it was observed that cyclohexanone linker played an important role in enhancing antifungal activity. Analogues with ethoxy (-OEt) group on the aromatic side-chain have better antifungal potential than other analogues having a methoxy (-OMe) and chloro (-Cl) group. Furthermore, antifungal potential is found to decrease when cyclopentanone and acetone were used as a linker molecule. Also, it was observed that most of the curcumin analogues showed strong potential against all fungal strains except *Cryptococcus neoformans*. In contrast, curcumin analogues **4g** and **4i** do not show significant antifungal activity against any tested pathogenic fungal strains, which also revealed that open space linker like acetone found to decrease antifungal activity.

In vitro antioxidant activity

All synthesised propargylated monocarbonyl curcumin analogues were further evaluated for in vitro radical scavenging activity. It was observed that the compound **4i** with acetone linker and 3,5-chloro substitution on the aromatic ring displayed potential antioxidant activity (IC_{50} = 12.78 ± 0.71) when compared with the standard drug BHT (IC_{50} = 16.47 ± 0.18) (Table 1). Furthermore, analogues **4b**, **4c** and **4e** displays almost greater or equal antioxidant potential as compared with BHT. Trends in antioxidant and antifungal activity data revealed that analogues **4b**, **4c** and **4e** exhibited potential antifungal and antioxidant activity as reflected in their *MIC* and IC_{50} values. Also, analogue **4i** which was inactive against fungal strains were found to exhibit strong antioxidant activity. It was observed that

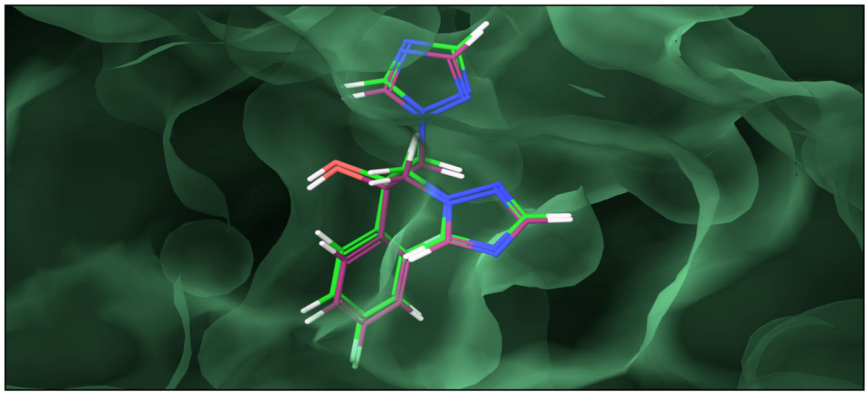

Fig. 5 Superimposition of the best scoring pose for Fluconazole obtained from docking (green carbon) against the X-ray bound conformation (pink carbon)

acetone linker enhances antioxidant activity than cyclic linker.

Molecular docking study

Promising levels of activities demonstrated by the propargylated monocarbonyl curcumin analogues investigated herein against the various fungal strains prompted us to carry out molecular docking studies against the crucial sterol 14α-demethylase (CYP51) enzyme (PDB code: 3KHM) to elucidate their plausible mechanism of antifungal activity. Within the framework of in silico structure-based drug design approaches, molecular docking has evolved an inevitable tool to predict the potential biological target with a substantial degree of accuracy especially in the absence of available resources to do the experimental enzyme assay. Sterol 14α-demethylase (CYP51) is an ancestral activity of the cytochrome P450 superfamily and is essential for ergosterol biosynthesis in fungi where it catalyzes the conversion of lanosterol to ergosterol. Inhibition of CYP51 leads to accumulation of 14α-methyl sterols and depletion of ergosterol in the fungal cell wall, resulting in altered cell membrane properties and function with subsequently increased permeability and inhibition of cell growth and replication.

Molecular docking protocol was validated by extracting the co-crystallised ligand (Fluconazole) and re-docking using the experimental set up described in the experimental part of docking analysis (Fig. 5).

From the ensuing docked conformations, it is revealed that all the propargylated monocarbonyl curcumin analogues could bind to the active site of CYP51 with varying degrees of affinities at co-ordinates close to the native structure by formation of a network of close interactions. The docking scores for the series varied from −8.939 for the most active to −7.088 for moderately active with an average docking score of −7.963 signifying a promising binding affinity towards CYP51. Furthermore, a detailed per-residue interaction analysis was carried out to identify the most significantly interacting residues and their associated thermodynamic interactions. This analysis is discussed in detail for one of the most active molecule **4a** and summarised in Table 2 for other active compounds **4b, 4c, 4f** and **4h** as well (SI-1 to SI-4, Supplementary Information).

The lowest energy docked conformation of **4a** (Fig. 6) revealed that it could snugly fit into the active site of CYP450 at co-ordinates similar to native ligand (Fig. 7) engaging in a network of bonded and non-bonded (steric and electrostatic) interactions.

The compound was found to be stabilised through most significant van der Waals interactions observed with Val461 (−3.246 kcal/mol), Phe290 (−2.953 kcal/mol), Ala287 (−2.954 kcal/mol), Glu205 (−2.741 kcal/mol), Tyr116 (−4.431 kcal/mol), Phe110 (−2.871 kcal/mol), Met106 (−3.155 kcal/mol), Tyr103 (−3.098 kcal/mol) residues *via* the central cyclohexanone nucleus while the 3-ethoxy-4-(prop-2-yn-1-yloxy) benzylidene side chains flanking both side of the nucleus engaged in similar van der Waals interactions with Hem500 (−5.738 kcal/mol), Met460 (−4.355 kcal/mol), Thr459 (−3.486 kcal/mol), Leu356 (−3.261 kcal/mol), Thr295 (−2.918 kcal/mol), Ala291 (−2.972 kcal/mol), Pro210 (−3.197 kcal/mol), Ile209 (−2.977 kcal/mol), Leu208 (−3.232 kcal/mol) and Ile105 (−3.288 kcal/mol) residues lining the active site. The enhanced binding affinity of **4a** is also attributed to very significant electrostatic interactions observed through Hem500 (−3.185 kcal/mol), Ile209 (−2.896 kcal/mol), Glu205 (−2.867 kcal/mol) and Tyr103 (−2.712 kcal/mol) residues.

Furthermore, **4a** also exhibited a very close hydrogen-bonding interactions with Tyr103(1.989 Å) residue through the ketone function of the central cyclohexanone nucleus which serve as an ″anchor″ to stabilise the 3D orientation of a ligand into the active site and also guide the steric and electrostatic (non-bonded) interactions. A similar network of bonded (H-bond) and non-bonded (steric and electrostatic) interactions were observed for other active analogues. It is noteworthy that all the active molecules,

Table 2 The per-residue interaction analysis based on docking study for propargylated monocarbonyl curcumin analogues with sterol 14α-demethylase (CYP51)

Code	Docking score	Glide interaction energy (kcal/mole)	Per-residues interactions	
			Coulombic (kcal/mol)	H-bond (Å)
4a	−8.939	−49.907	Hem500 (−3.185), Ile209 (−2.896), Glu205 (−2.867), Tyr103 (−2.712)	Tyr103 (1.989)
4b	−8.559	−48.324	Hem500 (−3.077), Ile209 (−2.596), Glu205 (−2.367), Tyr103 (−2.429)	–
4c	−8.097	−46.877	Hem500 (−2.939), Ile209 (−2.292), Glu205 (−2.349), Tyr103 (−2.392)	Tyr103 (2.088)
4f	−7.762	−47.954	Hem500 (−2.850), Ile209 (−2.196), Glu205 (−2.267), Tyr103 (−2.128)	Tyr103 (1.899)
4h	−7.637	−45.814	Hem500 (−2.739), Ile209 (−1.432), Glu205 (−2.139), Tyr103 (−2.092)	–
Fluconazole	−7.34	−52.92	Hem500 (−5.862), Ile209 (−2.896), Glu205 (−2.929), Tyr103 (−2.35)	Tyr116 (2.11)

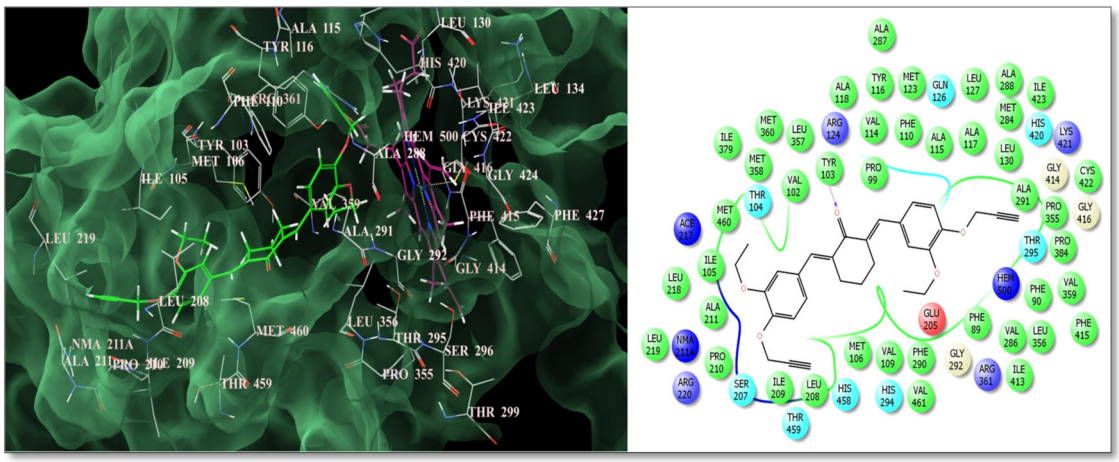

Fig. 6 Binding mode of **4a** into the active site of sterol 14α-demethylase (CYP51) (on the right side: the pink lines signify hydrogen-bonding interaction)

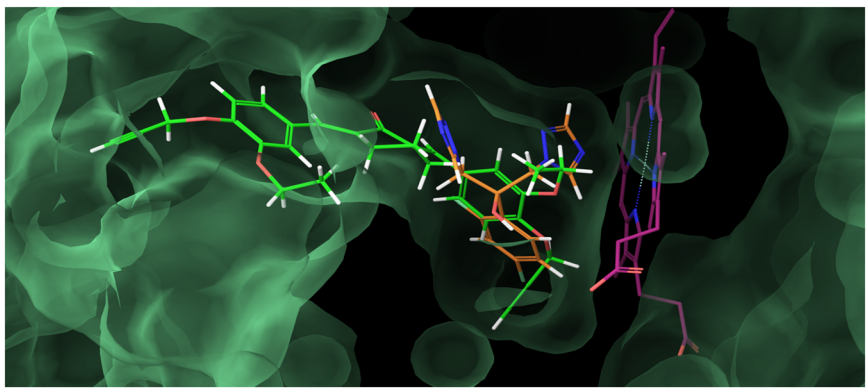

Fig. 7 Superimposition of the **4a** against the X-ray bound conformation of Fluconazole (Green backbone: **4a**, Orange backbone: Fluconazole; Pink backbone: Hem)

including **4a**, showed a very strong steric as well as electrostatic interaction with the Hem moiety (iron metal) of CYP51 which is crucial for antifungal activity knowing the experimental evidence that Miconazole is also coordinated with CYP51 through this Hem moiety. This suggests that the propargylated monocarbonyl curcumin analogues investigated herein may also exhibit their antifungal activity through CYP51 inhibition.

Materials and methods

General

All chemicals and reagents were procured from Sigma Aldrich, S.D. Fine chemical and commercial suppliers and used without further purification. TLC was performed on 0.25 mm E. Merck pre-coated silica gel plates (60 F_{254}). The components were identified by exposure to iodine vapours or UV light. The melting point was decided by using an open capillary technique and are uncorrected. The products were characterised using ^{1}H NMR, ^{13}C NMR spectra and MS. ^{1}H-NMR spectra were recorded in $CDCl_3$ on a Bruker DRX-400 MHz spectrometer. ^{13}C NMR spectra were recorded in $CDCl_3$ on a Bruker DRX-100 MHz instrument. TMS was used as the internal standard. IR spectra were recorded using a Bruker ALPHA ECO-ATR FTIR spectrometer. Mass spectra were recorded on LC/ESI-MS spectrometer.

General procedure for the preparation of prop-2-yn-1-yloxy benzaldehydes (2a–c)

An appropriate mixture of hydroxybenzaldehyde **1a–c** (1 mmol), propargyl bromide (1 mmol) and K_2CO_3 (2 mmol) in DMF (9–10 mL) was stirred at room temperature for 2–3 h. The progress of the reaction was monitored using TLC. After completion of the reaction, the reaction mixture was poured in ice-cold water. The separated solid was filtered washed with water, dried and recrystallised from ethanol resulted in the corresponding propargylated benzaldehydes in good yields (87–89%).

General procedure for the preparation of propargylated monocarbonyl curcumin analogues (4a–i)

A mixture of appropriate propargylated benzaldehydes **2a–c** (1 mmol), appropriate monoketone linker (1 mmol) and aq. NaOH in ethanol (10 mL) was stirred at room temperature for about 3–4 h. The progress of the reaction was monitored using TLC. The precipitate was washed with water, dried and recrystallised using ethyl acetate-chloroform as a solvent.

(2*E*,6*E*)-2,6-Bis(3-ethoxy-4-(prop-2-yn-1-yloxy)benzylidene) cyclohexanone (4a)

Yellow coloured crystal; yield 82%; mp: 150–153 °C; IR (KBr) ν_{max} 3262, 2120, 1660, 1589, 1503 cm^{-1}; ^{1}H NMR ($CDCl_3$, 400 MHz,): $\delta = 7.73$ (2H, s, Ar-C<u>H</u> = C-, H-3, H-3′), 7.08 (4H, s, Ar-H, H-5, H-5′, H-9, H-9′), 7.03 (2H, s, Ar-H, H-8, H-8′), 4.81 (4H, d, $J = 2.4$ Hz, Ar-OC<u>H</u>$_2$), 4.12 (4H, q, $J = 8.0$ Hz, -OC<u>H</u>$_2$CH$_3$), 2.93 (4H, t, $J = 8.0$ Hz, -C<u>H</u>$_2$-CH$_2$-C<u>H</u>$_2$), 2.53 (2H, d, $J = 2.4$ Hz, -C ≡ C<u>H</u>), 1.84–1.78 (2H, m, -CH$_2$-C<u>H</u>$_2$-CH$_2$), 1.47 (6H, t, $J = 8.0$ Hz, -OCH$_2$-C<u>H</u>$_3$); ^{13}C NMR ($CDCl_3$, 100 MHz,): $\delta = 190.1$ (C = O, C-1), 148.6 (Ar-C, C-7, C-7′), 147.6 (Ar-C, C-6, C-6′), 136.7 (Ar-<u>C</u>H = C-, C-3, C-3′), 134.8 (Ar-CH = <u>C</u>-, C-2, C-2′), 130.2 (Ar-C, C-4, C-4′), 123.5 (Ar-C, C-9, C-9′), 115.7 (Ar-C, C-8, C-8′), 114.2 (Ar-C, C-5, C-5′), 78.4 (-<u>C</u> ≡ CH-), 76.0 (-C ≡ <u>CH</u>-), 64.6 (-O<u>C</u>H$_2$), 56.8 (-O<u>C</u>H$_2$CH$_3$), 28.5 (-<u>C</u>H$_2$), 23.0 (-<u>C</u>H$_2$) and 14.8 (OCH$_2$-<u>C</u>H$_3$); HRMS: Calcd for $C_{30}H_{29}O_5$ $[M\text{-}H]^+$, 469.2093, found: 469.2143

(3*E*,5*E*)-3,5-Bis(3-ethoxy-4-(prop-2-yn-1-yloxy)benzylidene)-1-methylpiperidin-4-one (4b)

Yellow coloured crystal; yield 84%; mp: 152–154 °C; IR (KBr) ν_{max} 3241, 2117, 1660, 1574, 1502 cm^{-1}; ^{1}H NMR ($CDCl_3$, 400 MHz,): $\delta = 7.76$ (2H, s, Ar-C<u>H</u> = C-, H-3, H-3′), 7.11 (2H, d, $J = 8.4$ Hz, Ar-H, H-9, H-9′), 7.02 (2H, d, $J = 1.6$ Hz, Ar-H, H-5, H-5′), 6.99 (2H, d, $J = 8.4$ Hz, Ar-H, H-8, H-8′), 4.83 (4H, d, $J = 2.4$ Hz, Ar-OC<u>H</u>$_2$), 4.14 (4H, q, $J = 8.0$ Hz, -OC<u>H</u>$_2$CH$_3$), 3.80 (4H, s, -C<u>H</u>$_2$-N-C<u>H</u>$_2$-), 2.56 (2H, d, $J = 2.4$ Hz, -C ≡ C<u>H</u>), 2.5 (3H, s, -N-C<u>H</u>$_3$), 1.50 (6H, t, $J = 8.0$ Hz, -OCH$_2$-C<u>H</u>$_3$); ^{13}C NMR ($CDCl_3$, 100 MHz,): $\delta = 186.7$ (C = O, C-1), 148.8 (Ar-C, C-7, C-7′), 148.0 (Ar-C, C-6, C-6′), 136.3 (Ar-<u>C</u>H = C-, C-3, C-3′), 131.8 (Ar-CH = <u>C</u>-, C-2, C-2′), 129.5 (Ar-C, C-4, C-4′), 123.4 (Ar-C, C-9, C-9′), 115.8 (Ar-C, C-8, C-8′), 114.3 (Ar-C, C-5, C-5′), 78.4 (-<u>C</u> ≡ CH-), 76.1 (-C ≡ <u>CH</u>-), 64.6 (O<u>C</u>H$_2$-CH$_3$), 56.8 (Ar-O<u>C</u>H$_2$), 45.8 (-<u>C</u>H$_2$-N-<u>C</u>H$_2$), 29.7 (-N-<u>C</u>H$_3$), 14.8 (OCH$_2$-<u>C</u>H$_3$); LC-MS: Calcd for $C_{30}H_{32}NO_5$ $[M + H]^+$, 486.2, found: 486.2

(3*E*,5*E*)-3,5-Bis(3-methoxy-4-(prop-2-yn-1-yloxy) benzylidene)-1-methylpiperidin-4-one (4c)

Yellow coloured crystal; yield 80%; mp: 159–161 °C; IR (KBr) ν_{max} 3227, 2117, 1660, 1569, 1503 cm^{-1}; ^{1}H NMR ($CDCl_3$, 400 MHz,): $\delta = 7.75$ (2H, s, Ar-C<u>H</u> = C-, H-3, H-3′), 7.08 (2H, d, $J = 8.4$ Hz, Ar-H, H-9, H-9′), 7.01 (2H, d, $J = 1.2$ Hz, Ar-H, H-5, H-5′), 6.97 (2H, d, $J = 8.4$ Hz, Ar-H, H-8, H-8′), 4.81 (4H, d, $J = 2.4$ Hz, Ar-OC<u>H</u>$_2$), 3.90 (6H, s, -OC<u>H</u>$_3$), 3.78 (4H, s, -C<u>H</u>$_2$-N-C<u>H</u>$_2$-), 2.54 (2H, d, $J = 2.4$ Hz, -C ≡ C<u>H</u>), 2.48 (3H, s, -N-C<u>H</u>$_3$); ^{13}C NMR ($CDCl_3$, 100 MHz,): $\delta = 186.7$ (C = O, C-1), 149.3 (Ar-C, C-7, C-7'), 147.7 (Ar-C, C-6, C-6′), 136.2 (Ar-<u>C</u>H = C-, C-3, C-3′), 131.9 (Ar-CH = <u>C</u>-, C-2, C-2′), 129.4 (Ar-C, C-4, C-4′), 123.3 (Ar-C, C-9, C-9′), 114.3 (Ar-C, C-8, C-8′), 113.6 (Ar-C, C-5, C-5′), 78.1 (-<u>C</u> ≡ CH-), 76.2 (-C ≡ <u>CH</u>-), 57.1 (Ar-O<u>C</u>H$_2$), 56.6 (O<u>C</u>H$_3$), 56.0 (-<u>C</u>H$_2$-N-<u>C</u>H$_2$), 45.8 (-N-<u>C</u>H$_3$); LC-MS: Calcd for $C_{28}H_{28}NO_5$ $[M + H]^+$, 458.5, found: 458.5

(2*E*,5*E*)-2,5-Bis(3-ethoxy-4-(prop-2-yn-1-yloxy)benzylidene) cyclopentanone (4d)

Yellow coloured crystal; yield 81%; mp: 177–179 °C; IR (KBr) ν_{max} 3253, 2119, 1672, 1581, 1505 cm^{-1}; ^1H NMR ($CDCl_3$, 400 MHz,): $\delta = 7.53$ (2H, s, Ar-C<u>H</u> = C-, H-3, H-3′), 7.23 (2H, dd, $J = 8.4$ Hz and 1.6 Hz, Ar-H, H-9, H-9′), 7.15 (2H, d, $J = 1.6$ Hz, Ar-H), 7.11 (2H, d, $J = 8.4$ Hz, Ar-H), 4.83 (4H, d, $J = 2.4$ Hz, Ar-OC<u>H</u>$_2$), 4.15 (4H, q, $J = 7.2$ Hz, -OC<u>H</u>$_2$CH$_3$), 3.10 (4H, s, -C<u>H</u>$_2$), 2.53 (2H, d, $J = 2.4$ Hz, -C ≡ C<u>H</u>), 1.49 (6H, t, $J = 7.2$ Hz, -OCH$_2$-C<u>H</u>$_3$); ^{13}C NMR ($CDCl_3$, 100 MHz,): $\delta = 196.1$ (C = O, C-1), 148.9 (Ar-C, C-7, C-7′), 148.3 (Ar-C, C-6, C-6′), 135.8 (Ar-<u>C</u>H = C-, C-3, C-3′), 133.6 (Ar-CH = <u>C</u>-, C-2, C-2′), 130.2 (Ar-C, C-4, C-4′), 124.0 (Ar-C, C-9, C-9′), 115.6 (Ar-C, C-8, C-8′), 114.4 (Ar-C, C-5, C-5′), 78.3 (-<u>C</u> ≡ CH-), 76.1 (-C ≡ <u>C</u>H-), 64.7 (O<u>C</u>H$_2$-CH$_3$), 56.7 (Ar-O<u>C</u>H$_2$), 26.5 (-<u>C</u>H$_2$), 14.8 (OCH$_2$-<u>C</u>H$_3$); LC-MS: Calcd for $C_{29}H_{29}O_5$ $[M + H]^+$, 457.5, found: 457.2.

(2*E*,5*E*)-2,5-Bis(3-methoxy-4-(prop-2-yn-1-yloxy) benzylidene)cyclopentanone (4e)

Yellow coloured crystal; yield 83%; mp: 178–180 °C; IR (KBr) ν_{max} 3251, 2117, 1671, 1580, 1503 cm^{-1}; ^1H NMR ($CDCl_3$, 400 MHz,): $\delta = 7.78$ (2H, s, Ar-C<u>H</u> = C-, H-3, H-3′), 7.10 (2H, d, $J = 8.4$ Hz, Ar-H, H-9, H-9′), 7.03 – 6.98 (4H, m, Ar-H, H-5, H-5′, H-8, H-8′), 4.84 (4H, d, $J = 2.4$ Hz, Ar-OC<u>H</u>$_2$), 3.93 (6H, s, -OC<u>H</u>$_3$), 2.57 (2H, d, $J = 2.4$ Hz, -C ≡ C<u>H</u>), 2.50 (4H, s, -C<u>H</u>$_2$); ^{13}C NMR ($CDCl_3$, 100 MHz,): $\delta = 196.4$ (C = O, C-1), 149.1 (Ar-C, C-7, C-7′), 148.5 (Ar-C, C-6, C-6′), 136.0 (Ar-<u>C</u>H = C-, C-3, C-3′), 133.9 (Ar-CH = <u>C</u>-, C-2, C-2′), 130.4 (Ar-C, C-4, C-4′), 124.3 (Ar-C, C-9, C-9′), 115.8 (Ar-C, C-8, C-8′), 114.6 (Ar-C, C-5, C-5′), 78.5 (-<u>C</u> ≡ CH-), 76.4 (-C ≡ <u>C</u>H-), 64.8 (Ar-O<u>C</u>H$_2$), 56.8 (-O<u>C</u>H$_3$), 26.5 (-<u>C</u>H$_2$); ESI-MS: Calcd for $C_{27}H_{25}O_5$ $[M + H]^+$, 429.5, found: 430.0

(1*E*,4*E*)-1,5-Bis(3-ethoxy-4-(prop-2-yn-1-yloxy)phenyl)penta-1,4-dien-3-one (4f)

Yellow coloured crystal; yield 85%; mp: 144–146 °C; IR (KBr) ν_{max} 3263, 2120, 1645, 1579, 1502 cm^{-1}; ^1H NMR ($CDCl_3$, 400 MHz,): $\delta = 7.67$ (2H, d, $J = 16$ Hz, Ar-C<u>H</u> = C-, H-3, H-3′), 7.20 (2H, dd, $J = 8.4$ Hz and 2 Hz, Ar-H, H-9, H-9′), 7.16 (2H, d, $J = 2$ Hz, Ar-H, H-5, H-5′), 7.06 (2H, d, $J = 8.4$ Hz, Ar-H, H-8, H-8′), 6.95 (2H, d, $J = 16$ Hz, Ar-CH = C<u>H</u>-, H-2, H-2′), 4.82 (4H, d, $J = 2.4$ Hz, Ar-OC<u>H</u>$_2$), 4.15 (4H, q, $J = 7.2$ Hz, -OC<u>H</u>$_2$CH$_3$), 2.54 (2H, d, $J = 2.4$ Hz, -C ≡ C<u>H</u>), 1.50 (6H, t, $J = 7.2$ Hz, -OCH$_2$-C<u>H</u>$_3$); ^{13}C NMR ($CDCl_3$, 100 MHz,): $\delta = 188.8$ (C = O, C-1), 149.3 (Ar-C, C-7, C-7′), 149.2 (Ar-C, C-6, C-6′), 143.0 (Ar-<u>C</u>H = CH-, C-3, C-3′), 129.0 (Ar-C, C-4, C-4′), 124.0 (Ar-CH = <u>C</u>H-, C-2, C-2′), 122.5 (Ar-C, C-9, C-9′), 114.4 (Ar-C, C-8, C-8′), 112.2 (Ar-C, C-5, C-5′), 78.3 (-<u>C</u> ≡ CH-), 76.3 (-C ≡ <u>C</u>H-), 64.7 (O<u>C</u>H$_2$-CH$_3$), 56.8 (Ar-O<u>C</u>H$_2$), 14.9 (OCH$_2$-<u>C</u>H$_3$); LC-MS: Calcd for $C_{27}H_{27}O_5$ $[M + H]^+$, 431.5, found: 431.1

(1*E*,4*E*)-1,5-Bis(3-methoxy-4-(prop-2-yn-1-yloxy)phenyl) penta-1,4-dien-3-one (4g)

Yellow coloured crystal; yield 82%; mp: 155–157 °C; IR (KBr) ν_{max} 3253, 2109, 1660, 1571, 1495 cm^{-1}; ^1H NMR ($CDCl_3$, 400 MHz,): $\delta = 7.71$ (2H, d, $J = 16$ Hz, Ar-C<u>H</u> = C-, H-3, H-3′), 7.22 (2H, d, $J = 8.4$ Hz, Ar-H, H-9, H-9′), 7.17 (2H, s, Ar-H, H-5, H-5′), 7.07 (2H, d, $J = 8$ Hz, Ar-H, H-8, H-8′), 6.98 (2H, d, $J = 16$ Hz, Ar-CH = C<u>H</u>-, H-2, H-2′), 4.84 (4H, d, $J = 2.4$ Hz, Ar-OC<u>H</u>$_2$), 3.96 (6H, s, -OC<u>H</u>$_3$), 2.57 (2H, t, $J = 2.4$ Hz, -C ≡ C<u>H</u>); ^{13}C NMR ($CDCl_3$, 100 MHz,): $\delta = 188.6$ (C = O, C-1), 149.8 (Ar-C, C-7, C-7′), 149.0 (Ar-C, C-6, C-6′), 143.0 (Ar-<u>C</u>H = CH-, C-3, C-3′), 129.0 (Ar-C, C-4, C-4′), 124.0 (Ar-CH = <u>C</u>H-, C-2, C-2′), 122.5 (Ar-C, C-9, C-9′), 113.7 (Ar-C, C-8, C-8′), 110.5 (Ar-C, C-5, C-5′), 78.0 (-<u>C</u> ≡ CH-), 76.3 (-C ≡ <u>C</u>H-), 56.6 (Ar-O<u>C</u>H$_2$), 56.0 (O<u>C</u>H$_3$); LC-MS: Calcd for $C_{25}H_{23}O_5$ $[M + H]^+$, 403.4, found: 403.1

(2*E*,6*E*)-2,6-Bis(3,5-dichloro-2-(prop-2-yn-1-yloxy) benzylidene)cyclohexanone (4h)

Yellow coloured crystal; yield 84%; mp: 146–148 °C; IR (KBr) ν_{max} 3243, 2109, 1661, 1560, 1423 cm^{-1}; ^1H NMR ($CDCl_3$, 400 MHz,): $\delta = 7.87$ (2H, s, Ar-C<u>H</u> = C-, H-3, H-3′), 7.42 (2H, d, $J = 2.4$ Hz, Ar-H, H-7, H-7′), 7.22 (2H, d, $J = 2.4$ Hz, Ar-H, H-5, H-5′), 4.71 (4H, d, $J = 2.4$ Hz, Ar-OC<u>H</u>$_2$), 2.78 (4H, t, $J = 8.0$ Hz, -C<u>H</u>$_2$-CH$_2$-C<u>H</u>$_2$), 2.54 (2H, t, $J = 2.4$ Hz, -C ≡ C<u>H</u>), 1.82-1.76 (2H, m, -CH$_2$-C<u>H</u>$_2$-CH$_2$); ^{13}C NMR ($CDCl_3$, 100 MHz,): $\delta = 189.0$ (C = O, C-1), 151.3 (Ar-C, C-9, C-9′), 138.8 (Ar-<u>C</u>H = C-, C-3, C-3′), 133.3 (Ar-CH = <u>C</u>-, C-2, C-2′), 131.3 (Ar-C, C-7, C-7′), 130.2 (Ar-C, C-6, C-6′), 129.7 (Ar-C, C-5, C-5′), 129.5 (Ar-C, C-8, C-8′), 128.5 (Ar-C, C-4, C-4′), 77.8 (-<u>C</u> ≡ <u>C</u>H-), 61.0 (Ar-O<u>C</u>H$_2$), 28.5 (-<u>C</u>H$_2$), 22.7 (-<u>C</u>H$_2$); LC-MS: Calcd for $C_{26}H_{18}Cl_4O_3$ $[M]^+$, 520.2, found: 520.0

(1*E*,4*E*)-1,5-Bis(3,5-dichloro-2-(prop-2-yn-1-yloxy)phenyl) penta-1,4-dien-3-one (4i)

Yellow coloured crystal; yield 80%; mp: 181–183 °C; IR (KBr) ν_{max} 3285, 2126, 1664, 1599, 1554 cm^{-1}; ^1H NMR ($CDCl_3$, 400 MHz,): $\delta = 8.03$ (2H, d, $J = 16$ Hz, Ar-C<u>H</u> = C-, H-3, H-3′), 7.57 (2H, d, $J = 2.4$ Hz, Ar-H, H-7, H-7′), 7.45 (2H, d, $J = 2.4$ Hz, Ar-H, H-5, H-5′), 7.12 (2H, d, $J = 16$ Hz, Ar-CH = C<u>H</u>-, H-2, H-2′), 4.78 (4H, d, $J = 2.4$ Hz, Ar-OC<u>H</u>$_2$), 2.57 (2H, t, $J = 2.4$ Hz, -C ≡ C<u>H</u>); ^{13}C NMR

($CDCl_3$, 100 MHz,): $\delta = 188.4$ (C = O, C-1), 151.8 (Ar-C, C-9, C-9′), 136.9 (Ar-CH = CH-, C-3, C-3′), 132.3 (Ar-CH = CH-, C-2, C-2′), 131.7 (Ar-C, C-7, C-7′), 130.7 (Ar-C, C-6, C-6′), 129.8 (Ar-C, C-5, C-5′), 127.9 (Ar-C, C-8, C-8′), 125.9 (Ar-C, C-4, C-4′), 77.6 (-C ≡ CH-), 61.5 (Ar-OCH_2); ESI-MS: Calcd for $C_{23}H_{14}Cl_4KO_3$ $[M + K]^+$, 519.3, found: 520.0

Bioactivity assay

Antifungal activity assay

Standard agar dilution method as per CLSI (formerly, NCCLS) was used to determine in vitro antifungal activity of synthesised analogues (Collins 1967; Duraiswamy et al. 2009). Synthesised analogues and standard drug Miconazole were dissolved in DMSO solvent. A phosphate buffer solution of pH 7 was used to dissolve medium yeast nitrogen base furthermore, it was autoclaved at 110 °C for 10 min. A growth control without an antifungal agent and solvent control DMSO were included with each set. On Sabouraud dextrose agar, fungal strains were freshly subcultured and incubated at 25 °C for 72 h. Fungal cells were suspended and diluted to get 105 cells/mL in sterile distilled water. Ten microliters of standardised suspension were inoculated onto the control plates and the antifungal agents were integrated with the media. The inoculated plates were incubated at 25 °C for 48 h. At the end of 48 and 72 h readings were taken. The *MIC* values (Minimum inhibitory concentration of drugs preventing the growth of macroscopically visible colonies on drug-containing plates when there was visible growth on the drug-free control plates) was calculated.

Antioxidant activity assay

Synthesised curcumin analogues were screened for in vitro antioxidant activity by using 1, 1-diphenyl-2- picrylhydrazyl (DPPH) radical scavenging assay. The results were compared with standard antioxidant drug BHT (Butylated Hydroxy Toluene).

Radical scavenging activity of the synthesised compounds has been carried out in vitro by the 1, 1-diphenyl-2picrylhydrazyl (DPPH) radical scavenging assay (Burits and Bucar 2000). The obtained results were compared with standard antioxidant BHT (Butylated Hydroxy Toluene). The hydrogen atom or electron donation ability of the compounds was calculated from the bleaching of the purple-coloured methanol solution of 1, 1-diphenyl-1-picrylhydrazyl (DPPH). The spectrophotometric assay uses the stable radical DPPH as a reagent. 1 mL of various concentrations of the test compounds (5, 10, 25, 50 and 100 mg/mL) in methanol was added to 4 mL of 0.004% (w/v) methanol solution of DPPH. After a 30 min incubation period at room temperature, the absorbance was measured against blank at 517 nm. The percent inhibition (I %) of free radical production from DPPH was calculated by the following equation.

$$\% \text{ of scavenging} = [(\text{A control} - \text{A sample})/\text{A blank}] \times 100,$$

where 'A control' is the absorbance of the control reaction (containing all reagents except the test compound) and 'A sample' is the absorbance of the test compound. Tests were carried at in triplicate.

Molecular docking

To gauze the binding affinity and the mode of interaction of the new propargylated monocarbonyl curcumin analogues to the critical fungal enzyme sterol 14α-demethylase (CYP51), molecular docking study has been performed using the GLIDE (Grid-based Ligand Docking with Energetics) module of the Schrodinger Molecular modelling package (Schrodinger, LLC, New York, NY, 2015) (Halgren et al. 2004; Friesner et al. 2006). The 3D X-ray crystal structure of sterol 14α-demethylase (CYP51) complexed with its inhibitor-fluconazole (pdb code: 3KHM) was obtained from the Protein Data Bank (PDB) (http://www.rcsb.org/pdb) and cleaned using with the *protein preparation wizard* applying the OPLS-2005 force field. This includes deletion of the crystallographic water molecules as there are no conserved interactions with receptor; addition of the missing protons/side-chain atoms corresponding to pH 7.0 and assignment of the appropriate charge and protonation state. The refined structure thus obtained was subjected to energy minimisation to relieve the steric clashes among the amino acid residues till RMSD for the heavy atoms reached 0.30 Å. The 3D structures of the curcumin analogues were sketched using the *build* panel in *Maestro* and further optimised using *Ligand Preparation* tool. This involves adjusting realistic bond lengths and angles, assignment of the partial charges using the OPLS-2005 force-field followed by energy minimisation until the RMSD of heavy atoms reached 0.001 Å. Next, using the *Receptor Grid Generation* panel, shape and properties of the active site of the CYP51 enzyme were defined for which a grid box of 10 × 10 × 10 Å dimensions centred on the centroid of the co-crystallised ligand was generated. Before submitting the calculations for the synthesised dataset, the molecular docking protocol was validated by extracting the co-crystallised ligand (Fluconazole) and re-docking using the above setup which could produce an RMSD of <0.29 Å (Fig. 7).

With this setup, molecular docking was performed to determine the binding affinities and modes of binding of

the propargylated monocarbonyl curcumin analogues towards CYP51 using the extra precision Glide scoring function. The outputs files i.e. docking poses were visualised and investigated for the most significant elements of thermodynamic interactions using the Maestro's Pose Viewer utility.

Conclusion

In conclusion, we have synthesised a small, focused library of propargylated monocarbonyl curcumin analogues and screened for their in vitro antifungal and antioxidant activity. Most of the synthesised analogues especially **4a**, **4b** and **4c** were found to display excellent antifungal potential and can be further developed as lead molecules in search of new antifungal agents. Furthermore, the antioxidant activity of synthesised analogues was studied using DPPH assay and BHT as a positive control. Compound **4b**, **4c**, **4e** and **4i** displayed stronger antioxidant potential as compared with BHT. Furthermore, molecular docking study could provide valuable insight into the binding affinity and the mode of interactions of these compounds into the active site of crucial fungal enzyme CYP51. The per-residue interaction analysis could highlight the bonded (hydrogen bonding) and non-bonded (steric and electrostatic) interactions that influence their binding affinity towards the target. This information is being fruitfully utilised to optimise these propargylated monocarbonyl curcumin analogues to identify and optimise new antifungal and antioxidant agents.

Acknowledgements Author AAN is thankful to Principal, K. M. C. College Khopoli, for providing DST-FIST funded laboratory for this research work. Author SVA is very thankful to the Council of Scientific and Industrial Research (CSIR), New Delhi for providing a research fellowship. The authors are also grateful for providing laboratory facilities to the Head, Department of Chemistry, Dr Babasaheb Ambedkar Marathwada University, Aurangabad. We are also grateful to Schrodinger Inc. for GLIDE software to perform the molecular docking studies.

Compliance with ethical standards

Conflict of interest The authors declare that they have no conflict of interest.

Publisher's note Springer Nature remains neutral with regard to jurisdictional claims in published maps and institutional affiliations.

References

Ahmad W, Kumolosasi E, Jantan I et al. (2014) Effects of novel diarylpentanoid analogues of curcumin on secretory phospholipase A2, cyclooxygenases, lipo-oxygenase, and microsomal prostaglandin e synthase-1. Chem Biol Drug Des 83:670–681

Anand P, Kunnumakkara AB, Newman RA et al. (2007) Bioavailability of curcumin: problems and promises. Mol Pharm 4:807–818

Anand P, Thomas SG, Kunnumakkara AB et al. (2008) Biological activities of curcumin and its analogues (Congeners) made by man and mother nature. Biochem Pharmacol 76:1590–1611

Bairwa K, Grover J, Kania M, Jachak SM (2014) Recent developments in chemistry and biology of curcumin analogues. RSC Adv 4:13946–13978

Bodey GP (1992) Azole antifungal agents. Clin infect Dis 14: S161–S169

Buduma K, Chinde S, Dommati AK et al. (2016) Synthesis and evaluation of anticancer and antiobesity activity of 1-ethoxy carbonyl-3,5-bis (3′-indolyl methylene)-4-pyperidone analogs. Bioorg Med Chem Lett 26:1633–1638

Burits M, Bucar F (2000) Antioxidant activity of Nigella sativa essential oil. Phyther Res 14:323–328

Carapina da Silva C, Pacheco BS, das Neves RN et al. (2019) Antiparasitic activity of synthetic curcumin monocarbonyl analogues against Trichomonas vaginalis. Biomed Pharmacother 111:367–377

Casey PJ (1992) Biochemistry of protein prenylation. J Lipid Res 33:1731–1740

Chen SY, Chen Y, Li YP et al. (2011) Design, synthesis, and biological evaluation of curcumin analogues as multifunctional agents for the treatment of Alzheimer's disease. Bioorg Med Chem 19:5596–5604

Collins CH (1967) Microbiological methods. Butterworth-Heinemann, London

Da Silva CR, De Andrade Neto JB, De Sousa, Campos R et al. (2014) Synergistic effect of the flavonoid catechin, quercetin, or epigallocatechin gallate with fluconazole induces apoptosis in Candida tropicalis resistant to fluconazole. Antimicrob Agents Chemother 58:1468–1478

Deshmukh TR, Krishna VS, Sriram D et al. (2020) Synthesis and bioevaluation of α,α'-bis(1*H*-1,2,3-triazol-5-ylmethylene) ketones. Chem Pap 74:809–820

Duraiswamy B, Mishra S, Subhashini V et al. (2009) Studies on the antimicrobial potential of Mahonia leschenaultii Takeda root and root bark. Indian J Pharm Sci 68:389

Fine SA, Pulaski PD (1973) Reexamination of the Claisen-Schmidt condensation of phenylacetone with aromatic aldehydes. J Org Chem 38:1747–1749

Friesner RA, Murphy RB, Repasky MP et al. (2006) Extra precision glide: docking and scoring incorporating a model of hydrophobic enclosure for protein-ligand complexes. J Med Chem 49:6177–6196

Goel A, Kunnumakkara AB, Aggarwal BB (2008) Curcumin as "Curecumin": from kitchen to clinic. Biochem Pharmacol 75:787–809

Halgren TA, Murphy RB, Friesner RA et al. (2004) Glide: a new approach for rapid, accurate docking and scoring. 2. Enrichment factors in database screening. J Med Chem 47:1750–1759

Hatcher H, Planalp R, Cho J et al. (2008) Curcumin: from ancient medicine to current clinical trials. Cell Mol Life Sci 65:1631–1652

Kerru N, Singh P, Koorbanally N et al. (2017) Recent advances (2015–2016) in anticancer hybrids. Eur J Med Chem 142:179–212

Lal J, Gupta S, Thavaselvam D et al. (2016) Synthesis and pharmacological activity evaluation of curcumin derivatives. Chin Chem Lett 27:1067–1072

Li Y, Zhang LP, Dai F et al. (2015) Hexamethoxylated monocarbonyl analogues of curcumin cause G2/M cell cycle arrest in NCI-H460 cells via Michael acceptor-dependent redox intervention. J Agric Food Chem 63:7731–7742

Marchiani A, Rozzo C, Fadda A et al. (2013) Curcumin and curcumin-like molecules: from spice to drugs. Curr Med Chem 21:204–222

Martins CVB, Da Silva DL, Neres ATM et al. (2009) Curcumin as a promising antifungal of clinical interest. J Antimicrob Chemother 63:337–339

Masuda T, Maekawa T, Hidaka K, Bando H et al. (2001) Chemical studies on antioxidant mechanism of curcumin: analysis of oxidative coupling products from curcumin and linoleate. J Agric Food Chem 49:2539–2547

Nagargoje AA, Akolkar SV, Siddiqui MM et al. (2019) Synthesis and evaluation of pyrazole-incorporated monocarbonyl curcumin analogues as antiproliferative and antioxidant agents. J Chin Chem Soc 66:1658–1665

Nagargoje AA, Akolkar SV, Siddiqui MM et al. (2020) Quinoline based monocarbonyl curcumin analogs as potential antifungal and antioxidant agents: synthesis, bioevaluation and molecular docking study. Chem Biodivers 17(2):e1900624

Pappas PG, Kauffman CA, Andes DR et al. (2015) Clinical practice guideline for the management of candidiasis: 2016 update by the infectious diseases society of America. Clin Infect Dis 62:e1–e50

Paul NK, Jha M, Bhullar KS et al. (2014) All trans 1-(3-arylacryloyl)-3,5-bis (pyridin-4-ylmethylene)piperidin-4-ones as curcumin-inspired antineoplastics. Eur J Med Chem 87:461–470

Praditya D, Kirchhoff L, Bruning J et al. (2019) Anti-infective properties of the golden spice curcumin. Front Microbiol 10:912

Roman BI, De Ryck T, Verhasselt S et al. (2015) Further studies on anti-invasive chemotypes: an excursion from chalcones to curcuminoids. Bioorg Med Chem Lett 25:1021–1025

Sahu PK (2016a) Design, structure activity relationship, cytotoxicity and evaluation of antioxidant activity of curcumin derivatives/analogues. Eur J Med Chem 121:510–516

Sahu PK, Gupta SK et al. (2012) Synthesis and evaluation of antimicrobial activity of 4H-pyrimido[2,1-b] benzothiazole, pyrazole and benzylidene derivatives of curcumin. Eur J Med Chem 54:366–378

Sahu PK, Sahu PL, Agarwal DD et al. (2016b) Structure activity relationship, cytotoxicity and evaluation of antioxidant activity of curcumin derivatives. Bioorg Med Chem Lett 26:1342–1347

Sanabria-Rios DJ, Rivera-Torres Y, Rosario J et al. (2015) Chemical conjugation of 2-hexadecynoic acid to C5-curcumin enhances its antibacterial activity against multi-drug resistant bacteria. Bioorg Med Chem Lett 25:5067–5071

Seufert R, Sedlacek L, Kahl B et al. (2018) Prevalence and characterization of azole-resistant Aspergillus fumigatus in patients with cystic fibrosis: a prospective multicentre study in Germany. J Antimicrob Chemother 73:2047–2053

Shehaan DJ, Hitchcock CA, Sibley CA et al. (1999) Current and emerging azole antifungal agents. Clin Microbiol Rev 12:40–79

Shetty D, Kim YJ, Shim H, Snyder JP (2015) Eliminating the heart from the curcumin molecule: monocarbonyl curcumin mimics (MACs). Molecules 20:249–292

Singh H, Kumar M, Nepali K et al. (2016) Triazole tethered C 5 -curcuminoid-coumarin based molecular hybrids as novel anti-tubulin agents: design, synthesis, biological investigation and docking studies. Eur J Med Chem 116:102–115

Sokmen M, Khan A (2016) The antioxidant activity of some curcuminoids and chalcones. Inflammopharmacol 24:81–86

Subhedar DD, Shaikh MH, Nawale L et al. (2017) Quinolidene based monocarbonyl curcumin analogues as promising anti-mycobacterial agents: synthesis and molecular docking study. Bioorg Med Chem Lett 27:922–928

Tiwari A, Kumar S, Shivahare R et al. (2015) Chemotherapy of leishmaniasis part XIII: design and synthesis of novel heteroretinoid-bisbenzylidine ketone hybrids as antileishmanial agents. Bioorg Med Chem Lett 25:410–413

Wang YJ, Pan MH, Cheng AL, Lin LI, Ho YS, Hsieh CY et al. (1997) Stability of curcumin in buffer solutions and characterization of its degradation products. J Pharm Biomed Anal 15:1867–1876

Wang ZSen, Chen LZ, Liu XH, Chen FH (2017) Diarylpentadienone derivatives (curcumin analogues): synthesis and anti-inflammatory activity. Bioorg Med Chem Lett 27:1803–1807

Zheng QT, Yang ZH, Yu LY et al. (2017) Synthesis and antioxidant activity of curcumin analogs. J Asian Nat Prod Res 19:489–503

Ziani N, Sid A, Demonceau A et al. (2013) Synthesis of new curcumin analogues from Claisen-Schmidt condensation. Eur J Chem 4:146–148